Using Biomarkers to Improve Heavy Oil Reservoir Management: An Example From the Cymric Field, Kern County, California[1]

Mark A. McCaffrey,[2] Henry A. Legarre,[3] and Scott J. Johnson[4]

ABSTRACT

For biodegraded oil accumulations, field development can be optimized by using geochemical indicators of variations in the extent of bacterial alteration. Biodegradation typically reduces oil producibility by increasing oil viscosity. In the Cymric field (Kern County, California), sidewall core extracts reveal that the extent of oil biodegradation changes substantially over extremely short vertical distances in a shallow, low-permeability reservoir. Zones of more degraded oil can extend laterally for more than a mile. The relationships between oil viscosity and biomarker biodegradation parameters in this field were calibrated from analyses of produced oils, and these relationships were used to convert sidewall core biomarker analyses into quantitative predictions of lateral and vertical changes in oil viscosity and gravity. Compositional variations were also used to allocate production to discrete zones. Viscosity prediction and production allocation can be used to optimize (1) the placement of new wells, (2) the placement of completion intervals, (3) the thickness of steam injection intervals, and (4) the spacing between injection intervals in the same well.

INTRODUCTION

The economics of oil-field development are strongly affected by oil gravity and viscosity, which impact oil value and producibility, respectively. Studies of oils from throughout the world indicate that differences in oil gravity between either fields or reservoirs are controlled by source rock characteristics, such as thermal maturity and source rock type (e.g., Hunt, 1995), and by post-generation processes, such as (1) oil biodegradation, (2) evaporative fractionation during gas migration, (3) in-reservoir mixing of different oil types, and (4) water washing of oil (e.g., Milner et al., 1977; Thompson, 1987). However, for shallow oil accumulations, oil gravity and viscosity variations within a reservoir commonly are controlled primarily by variations in the degree of oil biodegradation, as illustrated by this study.

Biomarkers are molecular fossils present in oils and rock extracts and are commonly used in oil exploration to assess the origin, thermal maturity, and level of biodegradation of oils (e.g., Peters and Moldowan, 1993). Because different biomarkers have differing susceptibilities to bacterial alteration, biomarker distributions in oil can be used to quantify the extent to which the oil has been biodegraded (Peters and Moldowan, 1991). In this paper, we introduce a new technique for optimizing development and reservoir management of biodegraded oil accumulations using biomarker indicators of variations in oil biodegradation. Biomarker data from 80 sidewall cores and 17 oils in the Cymric field (Figure 1) are used to predict in-reservoir variations in oil viscosity and gravity. These compositional variations can be used to optimize well completion parameters (e.g., the placement of new wells and completion intervals) and to assess the relative production from discrete zones.

©Copyright 1996. The American Association of Petroleum Geologists. All rights reserved.

[1]Manuscript received August 30, 1995; revised manuscript received December 5, 1995; final acceptance February 8, 1996.

[2]Chevron Petroleum Technology Company, P.O. Box 446, La Habra, California 90633-0446. Present address: ARCO Exploration and Production Technology, 2300 West Plano Parkway, Plano, Texas 75075-8499.

[3]Chevron U.S.A. Production Company, P.O. Box 1392, Bakersfield, California 93302. Present address: Chevron Petroleum Technology Company, P.O. Box 446, La Habra, California 90633-0446.

[4]Chevron U.S.A. Production Company, P.O. Box 1392, Bakersfield, California 93302.

Editorial comments by B. J. Huizinga, K. E. Peters, L. K. Smith, J. E. Dahl, D. K. Baskin, S. Sanford, and M. Morea substantially improved the manuscript. Sidewall core extractions and preparation of the extracts for analysis by J. Jaime are gratefully acknowledged, as are GC-MS analyses and peak quantifications performed by P. A. Lipton and P. Guan, respectively.

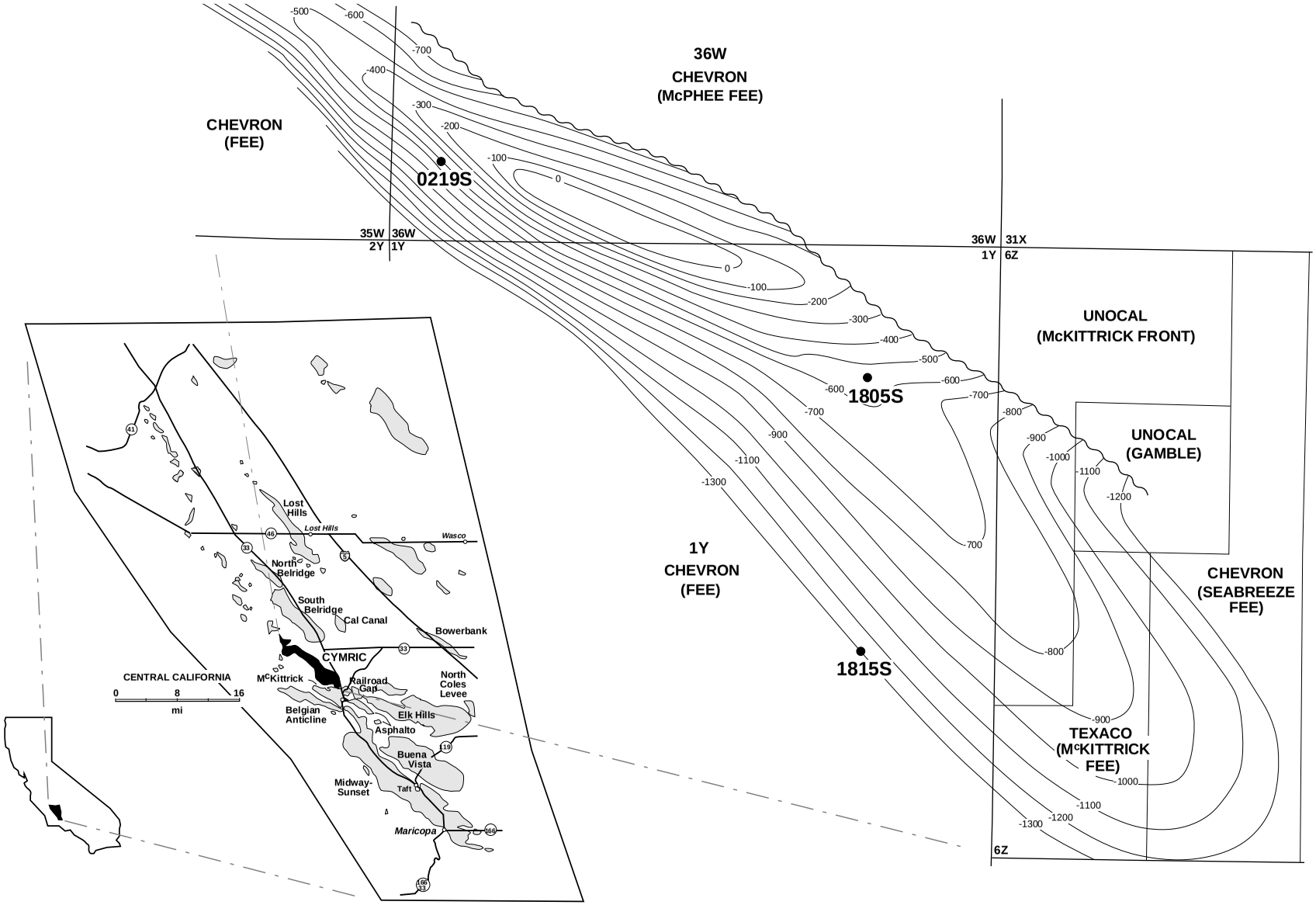

Figure 1—Inset map shows the Cymric field location. A portion of the Cymric field is shown in the larger map. The larger map shows the Cymric anticline contoured on the A5 horizon (Figure 2); also shown are the locations of wells 0219S, 1805S, and 1815S. Contour interval 100 ft.

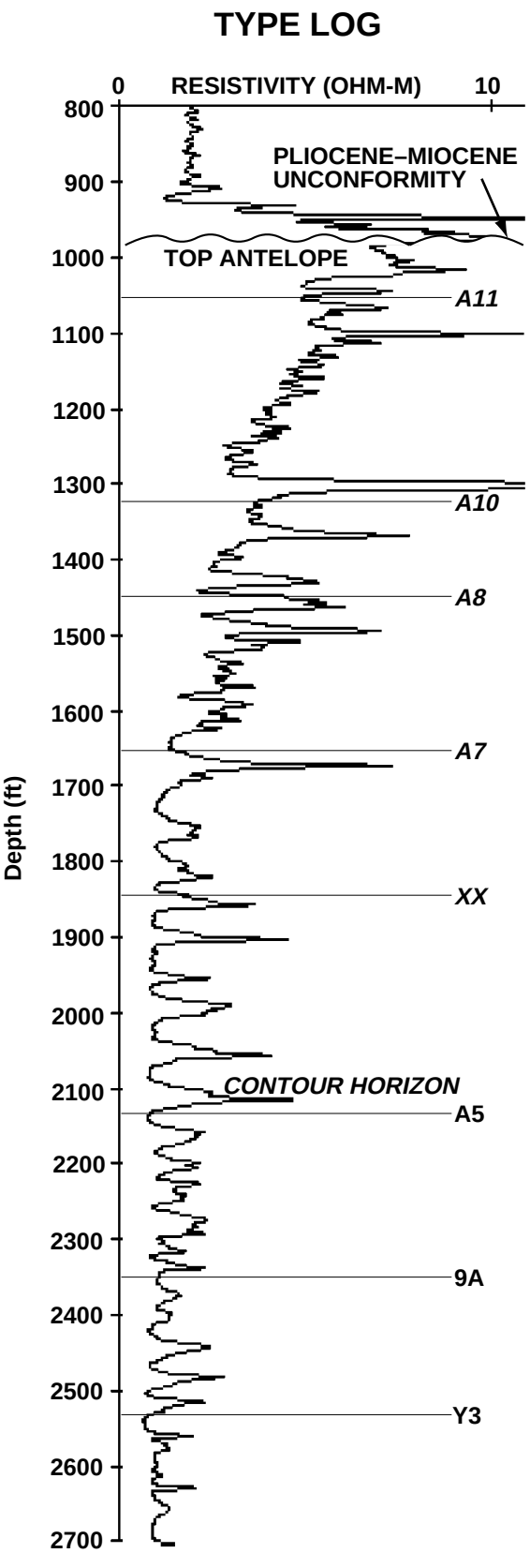

Figure 2—Type log for the Antelope reservoir.

DESCRIPTION OF THE FIELD AREA

Cymric field is located in the southwestern San Joaquin Valley, Kern County, California (Figure 1). The primary trap is a doubly plunging, northwest-trending anticline in section 1Y (Figure 1). This structure, one of a series of en echelon folds along the western margin of the San Joaquin Valley, formed in response to regional northeast-southwest compression associated with movement on the San Andreas fault (Graham and Williams, 1985). The primary reservoir, the Antelope Shale of the Miocene Monterey Formation, occupies the crest of the anticline and is a siliceous shale that is shallow (700–1600 ft or 200–500 m subsurface) and 600 ft (200 m) thick, with less than 1 md permeability and 40–60% porosity. This siliceous shale consists primarily of diatoms with varying proportions of sand, silt, and clay (Figure 2). The top of the reservoir is variably eroded and is bounded by the regional Pliocene–Miocene unconformity (Figure 2). Overlying shales of the Pliocene Etchegoin Formation provide a seal for the accumulation. Below the unconformity, the anticline is tightly folded, with Antelope Shale dips commonly exceeding 40°. Gentle folding of both the Pliocene–Miocene unconformity and the Monterey silica diagenetic boundaries along the anticline attest to late movements on this active structure.

At Cymric field, deep, synclinal Monterey Formation siliceous shales have generated oil that has accumulated in the shallower, thermally immature diatomite-porcellanite reservoir (Antelope Shale, >600 million bbl original oil in place). The gravity of the oil in the Antelope ranges from 8 to 18° API, and viscosity ranges from more than 7000 to less than 100 cp at 120°F. Oil saturations average approximately 50%. Deeper, volumetrically less important reservoirs containing Monterey-sourced oil occur in the field as deep as 4500 ft (1400 m). These accumulations have gravities as high as 25° API. Biomarker (molecular fossil) indicators of oil source and oil thermal maturity are essentially invariant in these reservoirs (e.g., mono- and triaromatic steroid distributions) (unpublished data). The degree of oil biodegradation [on a 0–10 scale developed by Peters and Moldowan (1993)] ranges from 6 (heavily degraded; complete loss of paraffins, acyclic isoprenoids, and most steranes) to 9 (very heavily degraded; complete loss of paraffins, acyclic isoprenoids, steranes, and hopanes) in the Antelope reservoir, and from 0 (nondegraded) to 5 (loss of paraffins and partial loss of isoprenoids) in the deeper accumulations of Monterey oil. Plots of oil viscosity vs. biomarker biodegradation parameters (discussed in following sections) indicate that variations in oil gravity and viscosity in this field are primarily controlled by the extent of biodegradation.

Table 1. Sidewall Sampling Depth and Bitumen Content

Well 0219S (elev. 894 ft)		Well 1805S (elev. 947 ft)		Well 1815S (elev. 944 ft)	
Measured Depth (ft)	Wt. % Oil	Measured Depth (ft)	Wt. % Oil	Measured Depth (ft)	Wt. % Oil
842	2.0	1003	11.4	1040	7.0
854	18.4	1095	18.5	1058	15.4
875	19.4	1140	24.1	1080	7.2
910	18.2	1164	26.3	1118	13.0
934	33.5	1190	32.3	1140	9.7
960	22.1	1200	25.4	1160	7.9
972	28.2	1255	21.3	1187	3.9
1026	31.6	1270	11.1	1200	6.5
1040	20.9	1330	32.1	1220	7.5
1103	26.6	1360	31.5	1250	5.4
1136	24.3	1380	28.3	1270	16.4
1150	15.5	1400	16.2	1290	13.5
1170	12.6	1410	28.7	1300	8.6
1184	12.4	1420	18.6	1320	11.5
1190	17.2	1430	15.3	1340	9.5
1202	14.0	1440	17.1	1350	7.4
1210	9.5	1450	2.1	1360	n.d.*
1222	5.2	1470	13.7	1430	15.3
1242	6.2	1480	4.1	1455	9.5
1250	9.0	1500	3.1	1500	8.0
1270	10.8	1530	11.7	1538	14.1
1300	13.6	1540	3.7	1570	1.1
1310	2.5	1550	2.0	1590	8.7
1322	10.5	1575	10.8	1610	3.2
1340	4.8	1580	1.4	1640	3.5
1353	8.0				
1374	5.8				
1393	1.4				
1446	5.1				
1515	2.2				

*n.d. = no data.

MATERIALS AND METHODS

The Antelope Shale reservoir samples are 80 sidewall cores from three Cymric wells (locations in Figure 1, depths in Table 1).

Microorganisms biodegrade different classes of compounds in petroleum at different rates (e.g., Peters and Moldowan, 1993). The early stages of oil biodegradation (loss of paraffins and isoprenoids) can be readily detected by gas chromatography (GC) analysis of an oil. However, in heavily degraded oils, such as those in Cymric, GC analysis alone cannot distinguish subtle differences in biodegradation due to interference of the unresolved complex mixture (UCM or "hump") that dominates the GC traces. Fortunately, in heavily degraded oils, one can use gas chromatography–mass spectrometry (GCMS) to quantify the concentrations of biomarkers with differing resistances to biodegradation. The UCM present on the GC trace of a heavily degraded oil does not affect this GC-MS analysis. In this study, we used GCMS analyses to distinguish vertical and lateral variations in the extent of oil biodegradation in the Antelope Shale.

Oil from each sidewall core (hereafter called "bitumens") was extracted using dichloromethane. Following solvent evaporation, the extracts were separated into asphaltene and maltene fractions by addition of hexane. The resulting maltene fractions were separated into saturated, aromatic, and polar fractions by high-pressure liquid chromatography (HPLC).

The saturated maltene fractions were analyzed by GCMS (scan runs to determine the concentrations of specific biomarkers) using a Hewlett Packard 5890 Series II gas chromatograph interfaced to a VG TRIO 1 quadrupole mass spectrometer. The GC column was a J&W fused silica capillary DB-1 column (60 m × 0.25 mm i.d., 0.25-μm methyl silicone film). The temperature program was isothermal for 5 min at 140°C, then increased

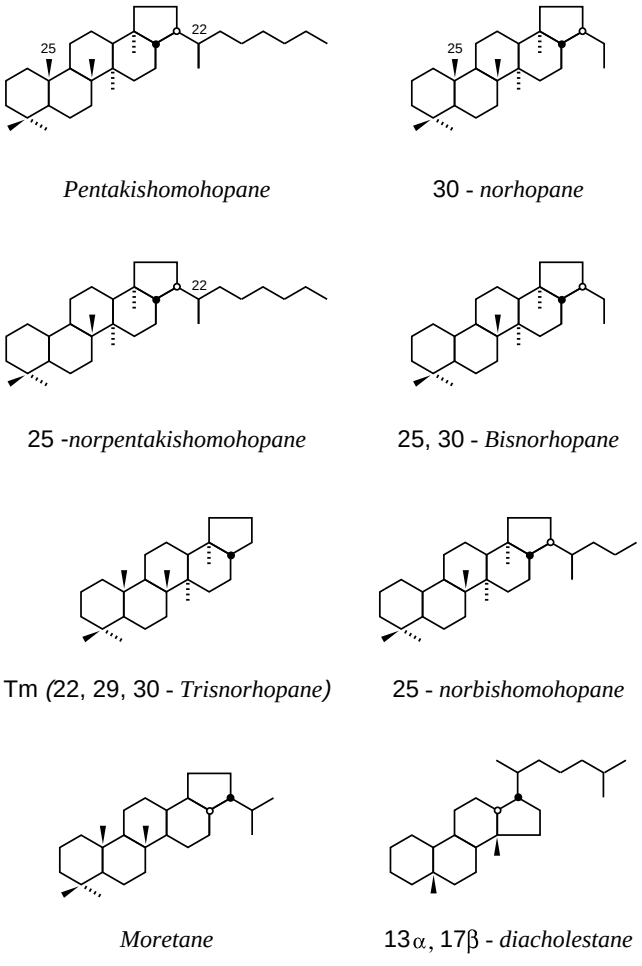

Figure 3—Structures of biomarkers discussed in text.

at 2°C/min to 320°C, and then isothermal at 320°C for 20 min. The injector temperature was 325°C, and the carrier gas was hydrogen. Hopanes were quantified from the m/z = 191 ion chromatograms, and 25-norhopanes were quantified from the m/z = 177 ion chromatograms. Most samples were analyzed twice, and the error bars shown in the figures represent ±1 standard deviation.

RESULTS

In all three wells (1815S and 1805S from section 1Y, and 0219S from section 36W, Figure 1), the entire 600-ft (200-m) oil column has been biodegraded (complete loss of paraffins, acyclic isoprenoids, and steranes). In wells 1805S and 1815S, the degree of oil biodegradation generally increases with depth. This trend can be seen by looking at variations with depth in the abundance of triterpanes, a specific group of compounds that microorganisms degrade after they have consumed the *n*-paraffins, acyclic isoprenoids, and steranes in an oil (Peters and Moldowan, 1993). 25-Norhopanes, a group of pentacyclic triterpanes, were especially useful in this study (Figure 3 provides the structures of compounds discussed in the text). These compounds are produced by the bacterial alteration of hopanes, another group of triterpanes (Seifert and Moldowan, 1979; Volkman et al., 1983; Requejo and Halpern, 1989; Peters and Moldowan, 1991; Peters et al., 1994; Moldowan and McCaffrey, 1995); the concentration of 25-norhopanes increases as hopanes are degraded. In the samples from wells 1805S and 1815S, 25-norhopanes generally increase in abundance down hole, indicating a progressive increase in biodegradation with depth. Similarly, the hopanes generally decrease in abundance with depth.

Biodegradation trends correlate between wells. Concentration profiles of a particular type of 25-norhopane in the extracts from each well are plotted structurally (i.e., relative to sea level) in Figure 4. In all of the wells, a zone of slightly more degraded oil [~100 ft (~ 30 m) thick, centered at about –594 ft (–181 m) subsea depth] is present near the bottom of the oil column. This conclusion is indicated by the maximum in each 25-norpentakishomohopane concentration profile at this depth (in Figure 4, the subsea depths are shown on the tie lines, and the measured depths are shown on the Y-axes of the well profiles). Correlation of the biodegradation profiles on this structural cross section indicates that the extent of biodegradation in this field is a function of depth rather than of stratigraphy. The different depths of the "XX" stratigraphic marker in each well in Figure 4 indicate that the extent of biodegradation crosscuts stratigraphy. A second zone of slightly more degraded oil is present at –66 ft (–20 m) subsea in well 0219S, but not in the other two wells. Similarly, a third zone of slightly more degraded oil is present at –376 ft (–115 m) subsea in well 1815S, but not in the other two wells. These vertical variations in the extent of biodegradation are also detectable on profiles of the concentration of hopanes in these samples. Because hopanes are converted to 25-norhopanes during oil biodegradation, a minimum on a hopane profile and a corresponding maximum on a 25-norhopane profile indicate a higher degree of biodegradation.

The timing of the oil biodegradation (i.e., whether the biodegradation is an ancient or a continuing process) and the effects of reservoir properties on the bacterial alteration are uncertain. The variations in biodegradation between wells may be a function of the intensity of natural fracturing. The causes for the variations in oil biodegradation with depth are not known, although they may reflect differences in either residual water saturation or access to

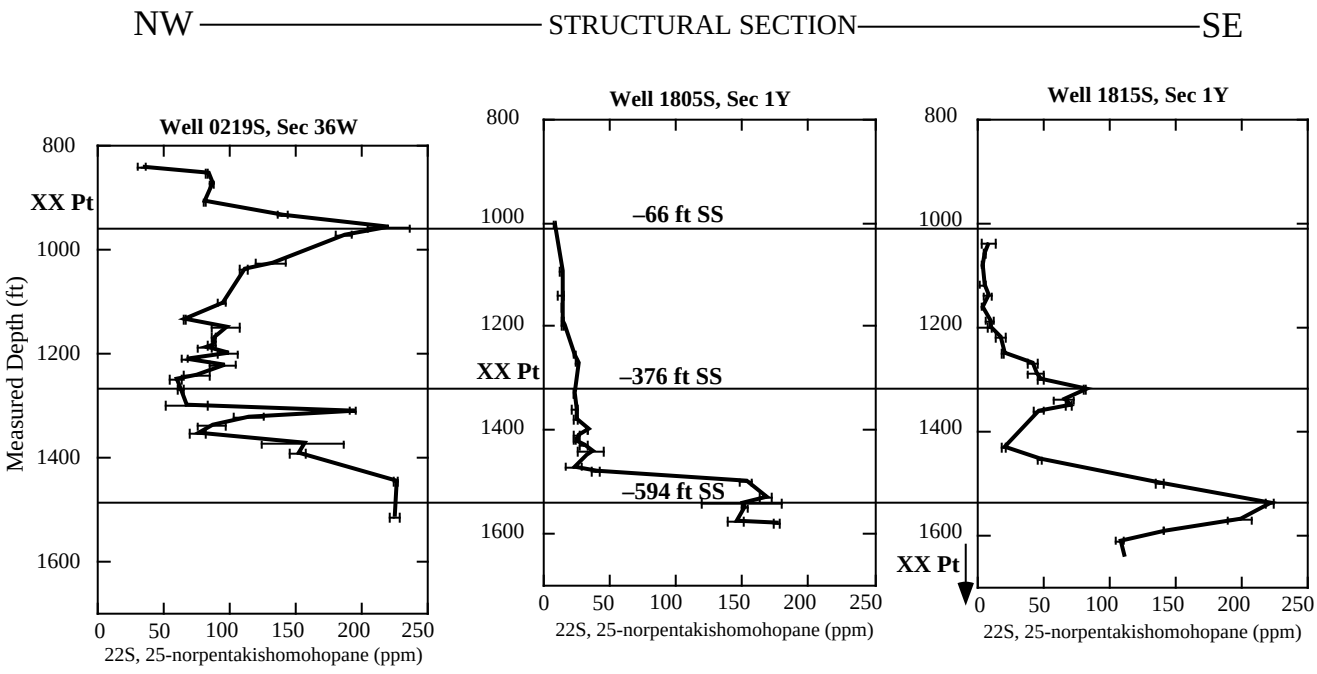

Figure 4—The abundance of 25-norpentakishomohopane (22S) in sidewall core extracts (as ppm saturate fraction). The profiles are arranged as a structural section relative to sea level. Subsea depths are shown on the three tie lines, and measured depths are shown on the Y-axes of the well profiles. A stratigraphic marker, the XX point (Figure 2), occurs at measured depths of 915, 1304, and 1870 ft (estimate) (279, 397, 570 m) in wells 0219S, 1805S, and 1815S, respectively. The positions of the XX point in the wells illustrate that the zone of more degraded oil at –594 ft (–181 m) subsea (bottom tie line) crosscuts stratigraphy.

meteoric water. In some cases, changes in relative permeability caused by silica phase changes may affect the rate of bacterial alteration. The extent of biodegradation appears unrelated to the amount of oil in place. The low reservoir permeability (<1 md), low oil gravity (~8–18° API), and low vertical permeability of this 600-ft (180-m) oil column are probably responsible for preserving the vertical variations in the oil chemistry; in-situ reservoir mixing of oil has probably proceeded too slowly (relative to the rate of biodegradation) to homogenize the oil column.

For this field, we calibrated the relationship between biomarker biodegradation parameters and oil viscosity. We analyzed biomarker distributions, oil viscosity, and oil gravity for 15 produced Cymric oils that cover the range of viscosities (Figure 5) encountered in Monterey-sourced oils from this field. Relationships derived from these produced oils allowed us to assess the magnitude of variations in gravity and viscosity represented by fluctuations in the sidewall core biomarker profiles.

Among the measured biomarker parameters, the C_{35} homohopane index (C_{35} homohopanes/ΣC_{31}–C_{35} homohopanes) correlates best with viscosity (Table 2, Figure 6). The denominator of this index is the sum of a group of ten homohopanes, whereas

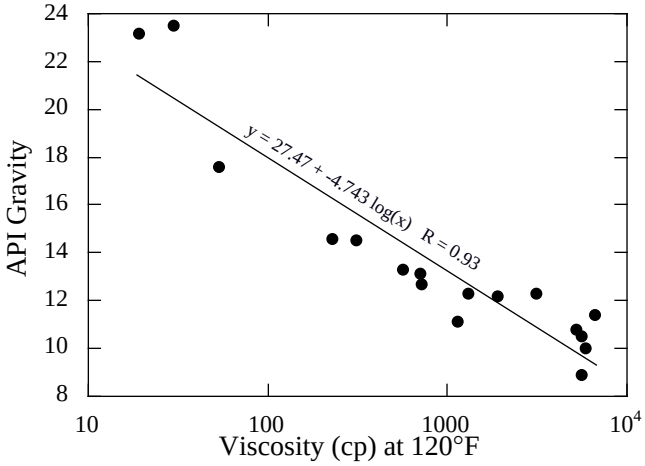

Figure 5—Oil gravity vs. viscosity in produced oils from the Cymric field. The regression shown includes all the data. If the two highest gravity samples are excluded, the best fit becomes gravity = 22.37 – 3.213 log (viscosity at 120°F), which has a correlation coefficient of 0.93.

the numerator is the sum of the two compounds in this group that are relatively more resistant to biodegradation (Moldowan and McCaffrey, 1995). Therefore, as biodegradation increases (and causes

Table 2. Correlations Between Viscosity and Selected Compositional Parameters for 15 Cymric Field Oils

Biomarker Parameter (Y)	Linear Regression of Cross Plot with Viscosity (at 120°F)	Correlation Coefficient (r)
Homohopane Index (i.e., C_{35} homohopanes/sum of C_{31} to C_{35} homohopanes)	$Y = 0.095432 + 0.000038349 \times$ (viscosity)	0.88
25-nortrishomohopane (22R)/trishomohopane (22R)	$Y = 0.50471 + 0.00076907 \times$ (viscosity)	0.88
25,30-bisnorhopane/30-norhopane	$Y = 1.387 + 0.0025189 \times$ (viscosity)	0.82
(Σ C_{31} to C_{33} 25-norhopanes)/(C_{28} + C_{29} tricyclic terpanes)	$Y = 1.8993 + 0.00059147 \times$ (viscosity)	0.82
(T s+ Tm)/(C_{32} + C_{33} hopanes)	$Y = 0.73126 + 0.00048213 \times$ (viscosity)	0.78
(C_{28} + C_{29} tricyclic terpanes)/(C_{32} + C_{33} hopanes)	$Y = 0.63341 + 0.00041721 \times$ (viscosity)	0.76
(C_{28} + C_{29} tricyclic terpanes)/(Σ C_{29} to C_{35} hopanes)	$Y = 0.14371 + 0.000080069 \times$ (viscosity)	0.76
25-norhopane/hopane	$Y = 3.2443 + 0.0030953 \times$ (viscosity)	0.76
(Σ C_{30} to C_{34} 25-norhopanes)/(Σ C_{31} to C_{35} homohopanes)	$Y = 0.69273 + 0.00093135 \times$ (viscosity)	0.75
(wt. % asphaltic material)/(wt. % saturated + aromatic fractions)	$Y = 0.76322 + 0.000075764 \times$ (viscosity)	0.74

viscosity to increase) the C_{35} homohopane index increases. The compound ratio 22R,25-nortrishomohopane/22R-trishomohopane also shows a strong correlation to viscosity (Figure 7). This correlation exists because the compound in the denominator is converted by biodegradation into the compound in the numerator (Moldowan and McCaffrey, 1995).

Using the equations for linear regressions through the data in Figures 6 and 7, we calculated viscosity profiles for well 1815S from sidewall core extract biomarker data. This approach revealed substantial viscosity variations (thousands of centipoise at 120°F) with depth in the Antelope reservoir (Figure 8). Differences between the two viscosity profiles in Figure 8 reflect the imperfect correlations between the biomarker and viscosity data used to construct the equations in Table 2, which is why certain samples have negative viscosities in Figure 8. These differences suggest that the viscosity profiles can best be used to estimate the magnitude of viscosity fluctuations in this oil column, rather than the absolute viscosity of any given point.

FIELD DEVELOPMENT AND RESERVOIR MANAGEMENT APPLICATIONS

Identifying Zones of High and Low Producibility

Depending on the starting composition of an oil, biodegradation can either increase or decrease oil viscosity. For certain very waxy crudes, the early stages of biodegradation can lower oil viscosity by removing high-molecular-weight paraffins (Colling and Robison, 1991). However, light biodegradation of oils rich in polar material (such as nitrogen-, oxygen-, and sulfur-containing resins and asphaltenes) or moderate to heavy biodegradation of any oil type increases oil viscosity and lowers API gravity by enriching the less easily degraded polar components in the residual oil (e.g., Miller et al., 1987; Colling and Robison, 1991).

Previous researchers have constructed transforms that relate biomarker distributions in nondegraded oils to oil gravity so that the original gravity of biodegraded oils (i.e., the gravity before biodegradation) could be inferred from the degradation-resistant biomarkers in the degraded oils (Hughes and Holba, 1988; Moldowan et al., 1992). The problem we address here is conceptually different: We illustrate how the present gravity (or viscosity) of

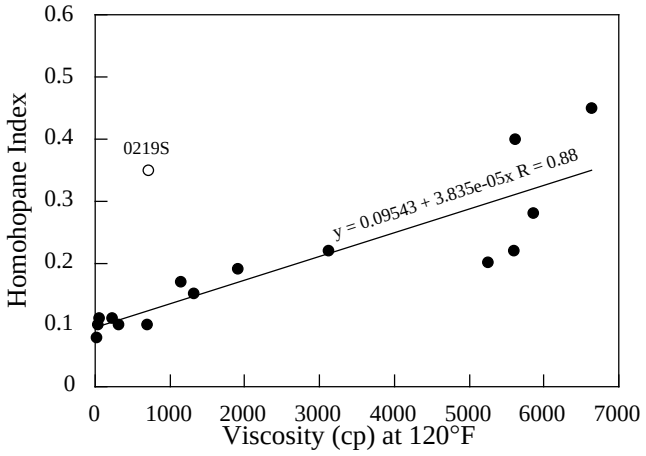

Figure 6—Viscosity vs. homohopane index in Cymric field produced oils. The regression excludes the oil from the 0219S well, which has an unusually large saturated hydrocarbon fraction and may represent an oil fractionated by the enhanced oil recovery process. The equation calculated here is used in Figure 8 to estimate oil viscosities from sidewall core extracts from the 1815S well.

biodegraded oils can be predicted from the distribution of biodegradation-sensitive biomarkers in rock extracts. We are unaware of any previous research that has calibrated the relationship between biodegradation parameters and either gravity or viscosity. Such calibrations would probably have to be field specific because they would depend on the starting composition of the oil and the consortia of bacteria active in a given reservoir.

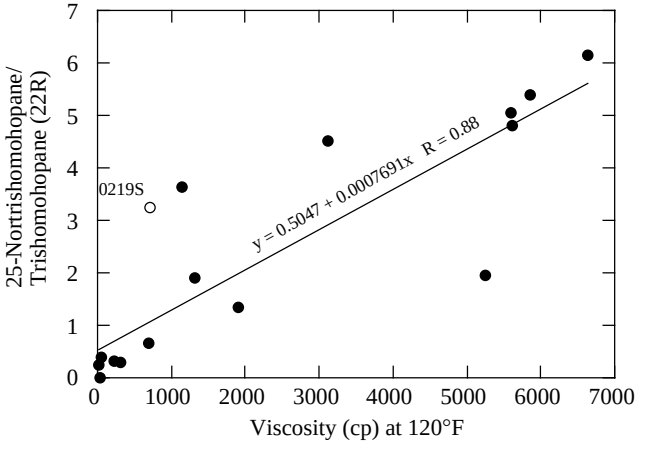

Figure 7—Viscosity vs. 25-nortrishomohopane/trishomohopane in Cymric field produced oils. The regression excludes the oil from the 0219S well, which has an unusually large saturated hydrocarbon fraction and may represent an oil fractionated by the enhanced oil recovery process. The equation calculated here is used in Figure 8 to estimate oil viscosities from sidewall core extracts from the 1815S well.

In cases where oil viscosity varies with depth in a reservoir, oil viscosity profiles are extremely valuable in optimizing field development. Typically, oil samples from production tests or repeat formation tester (RFT) tools cannot be obtained with sufficient vertical resolution to construct detailed viscosity or gravity profiles. In contrast, oil samples with very high vertical resolution can be obtained by solvent extraction of core or sidewall cores from reservoirs. Furthermore, sidewall cores are far less expensive to obtain than oil samples from production tests or an RFT tool. However, neither oil viscosity nor API gravity can be readily measured from reservoir core because the solvent used to extract oil from rock alters the oil viscosity and gravity. This problem is solved by measuring a property in the sidewall core extracts that can be related to oil viscosity by means of a mathematical transform. This approach was used by Baskin and Jones (1993), who defined a relationship between oil sulfur content and oil gravity to estimate oil viscosity and gravity from Monterey Formation sidewall cores in offshore California. However, their approach is applicable only to fields where oil viscosity is a function of oil thermal maturity. In oil accumulations where the viscosity is controlled primarily by biodegradation, sulfur content does not vary sufficiently with oil gravity to provide a useful sulfur-gravity or sulfur-viscosity relationship (Baskin and Jones, 1993). As a result, our study used biomarker-viscosity relationships to predict viscosity.

Although oil gravities in the Cymric field range from 8° to 24° API, spatial variations of oil in the 10–14° API gravity range are especially important in this field. Most of the oil in the diatomite-porcellanite is in this gravity range, and oil viscosity (and hence producibility) changes radically from 10° to 14° API (Figure 5). For well 1815S, the calculated oil viscosity profiles (Figure 8) are characterized by two maxima: one from 1300–1350 ft (396–412 m) and one below 1430 ft (436 m). Both maxima have calculated viscosities (from the biomarker data) that are thousands of centipoise greater (at 120°F) than the viscosity of the oil immediately above and below each maximum. The viscosity of the deeper maximum cannot be calculated for several samples deeper than 1455 ft (444 m) because oil biodegradation has entirely removed the biomarkers used to calculate the viscosity. Presumably, the oil at those depths is even more viscous than that at shallower depths in the reservoir.

These results suggest that mapping biodegradation indicators is a way to predict lateral and vertical variations in oil viscosity. Because oil viscosity

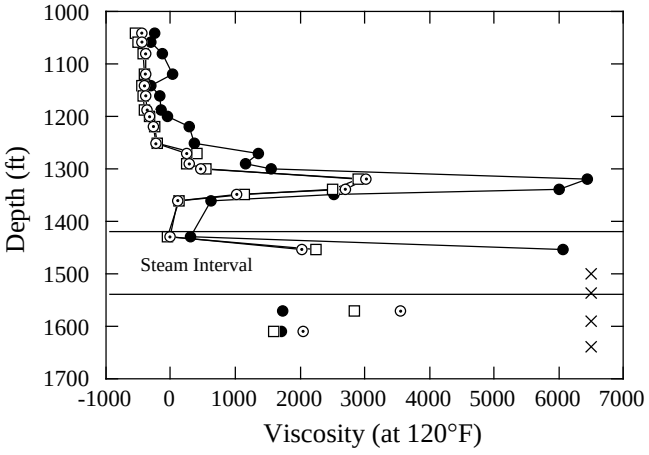

Figure 8—Well 1815S, section 1Y (Figure 1). Viscosities calculated from sidewall core biomarker data using the first three equations in Table 2. The black circles show the oil viscosities calculated from the homohopane index data (i.e., using the Figure 6 calibration). The open squares show the oil viscosities calculated from the 22R,25-nor-trishomohpane/22R-trishomohopane data (i.e., using the Figure 7 calibration). The open circles show the oil viscosities calculated from the 25,30-bisnorhopane/30-norhopane data (i.e., using the third equation in Table 2). X shows the depths of sidewall cores with viscosities that cannot be calculated because the homohopanes have been entirely degraded in these samples.

directly affects oil producibility, predicting variations in oil viscosity could impact selection of completion intervals in new wells and recompletion intervals in existing wells.

Production Allocation

In high-permeability reservoirs containing nondegraded oil, the oil within a given reservoir compartment is typically compositionally homogeneous, a fact that allows reservoir compartmentalization to be identified from oil geochemistry (e.g., Kaufman et al., 1990; Hwang and Baskin, 1994; Hwang et al., 1994). In such settings, allocation of commingled production to discrete pay zones is relatively straightforward. If oils from two compartments, oils I and II, are being commingled, then the percentage of oil I in the commingled production can be calculated as

$$\%I = \frac{\left(C_{II} - C_{mix}\right)\times 100}{\left(C_{II} - C_{I}\right)} \qquad (1)$$

where C_{II} is the concentration of a given compound in oil II, C_I is the concentration of the same compound in oil I, and C_{mix} is the concentration of the compound in the commingled oil. A graphical approach based on this type of simple mixing model was used by Schoell et al. (1993) to allocate commingled gas production.

In the case of a heavily biodegraded oil column (such as that in the Antelope Shale at Cymric) that changes in composition with depth, an assessment of which portions of the reservoir are yielding production requires assessing the contributions of multiple end members. Although equation 1 only allows one to assess the contributions of two end members to commingled production, we can extend this approach to include multiple end members by using matrix algebra. Consider the following hypothetical example. The concentration

	Extract 1	Extract 2	Extract 3	Extract 4
ppm compound A	5	10	1	3
ppm compound B	10	6	3	2
ppm compound C	8	4	1	1
ppm compound D	1	4	5	7

= Matrix G

Produced oil

ppm compound A	3.5
ppm compound B	5.2
ppm compound C	3.4
ppm compound D	4.1

= Matrix d

Fraction contributed by interval 1	0.3
Fraction contributed by interval 2	0.1
Fraction contributed by interval 3	0.4
Fraction contributed by interval 4	0.2

= Matrix M

Figure 9—Hypothetical production allocation problem discussed in text. The concentration of four compounds (A, B, C, and D) in sidewall core extracts are expressed as matrix G. The same four compounds are measured in a produced oil and expressed as matrix d. If the produced oil came only from some combination of production from the four intervals sampled by the sidewall cores, then (using equation 2) the relative contributions from the four intervals could be determined as matrix M (see Appendix 1).

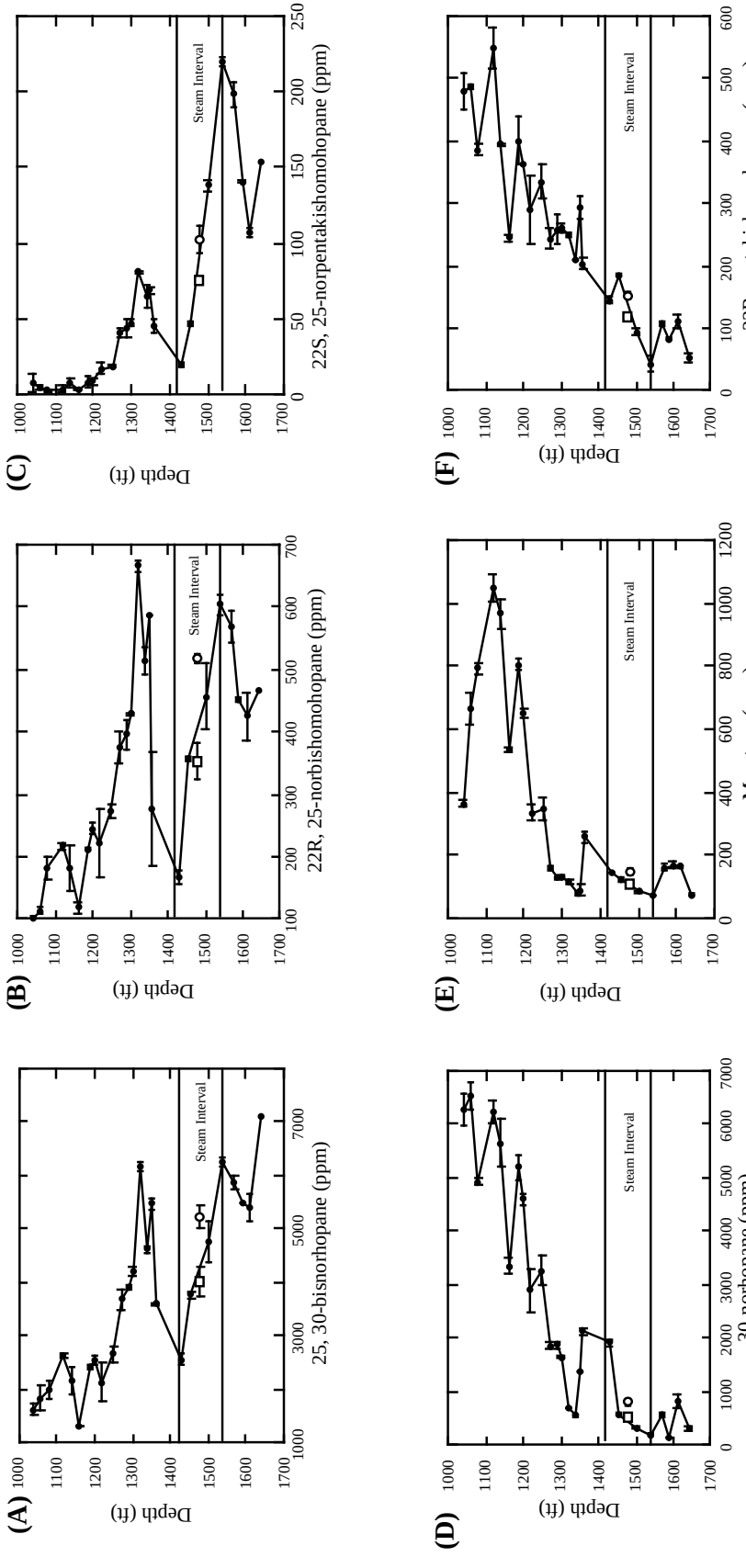

Figure 10—Concentrations (in ppm of saturated hydrocarbon fraction) of six biomarkers in sidewall core extracts (black circles) and two produced oils [shown at 1479 ft (451 m); the open square is the first produced oil; the open circle is the second produced oil] from well 1815S. The steam injection interval is indicated with horizontal bars. Error bars indicate one standard deviation calculated from nonconsecutive duplicate analyses of each sample. Differences between biomarker profiles allow unique fingerprints to be constructed for discrete depth intervals. These fingerprints can then be used to assess the origin of the produced oil.

of four compounds (A, B, C, and D) are measured in sidewall core extracts from four zones that may be contributing to a produced oil. These data can be expressed as a 4×4 matrix (matrix G, Figure 9) where the numbers are compound concentrations in parts per million (ppm). If the same four compounds were measured in a produced oil, then another matrix (matrix d, Figure 9) could be used to express the composition of the produced oil. If the produced oil came only from some combination of production from the four intervals sampled by the sidewall cores, then the relative contributions from the four intervals could be readily determined (matrix M, Figure 9) because

$$M = \left[G^T G\right]^{-1} G^T d \qquad (2)$$

where G^T is the transpose of matrix G. However, we are constrained by the following: the number of potentially identifiable producing zones cannot exceed the number of unique compound profiles used to construct the fingerprint of each oil (i.e., the number of variables must be less than or equal to the number of equations). If the number of rows (compounds) in matrix G is less than the number of columns (extracts), then no solution to the problem can be identified. However, the form in which equation 2 is written does allow the number of compounds to exceed the number of extracts. Equation 2 can be readily solved using the built-in functions in Microsoft EXCEL®, as described in Appendix 1.

During development of heavy-oil-containing, low-permeability reservoirs, the ability to allocate production to specific portions of a reservoir could favorably impact the choice of well-completion strategies (such as the spacing of hydrofracturing or steam cycling intervals) or values for enhanced oil recovery parameters (such as steam injection rates).

The wells examined in this study produce oil by a three-step process: (1) steam is injected into a specific depth interval [~80–120 ft (~24–37 m) thick] for several days, (2) the well is temporarily shut in to "soak," and then (3) is put on flowing production for several weeks. This process is then repeated with steam injected into the same interval. Ideally, after several cycles, the interval becomes depleted of producible oil. The well is subsequently recompleted uphole, where the cyclic steaming is continued. A key question associated with this process is the relationship between the steamed interval and the effective producing zone (i.e., does the entire steamed interval produce, or is part of the production from below or above the injection interval). Which interval yields production is a function of porosity and permeability, the geometry of the fracture network induced by the steam injection, and spatial variations in the producibility of the oil. In some instances, high-permeability intervals acting as "thief" zones preclude the development of induced fractures and hence restrict the dimensions of the producing interval.

Cyclic steam processing is not selectively producing one chemical fraction of the oil in place. For example, in wells 1805S and 1815S the bulk composition of the produced oils (i.e., wt. % saturated compounds, wt. % aromatic compounds, wt. % polar compounds) does not differ from the bulk composition of the sidewall core extracts. Therefore, vertical variations in the extent of oil biodegradation can be used to tie production from these wells to specific reservoir intervals. This may not be true for the oil sample from well 0219S (e.g., Figures 6 and 7).

Using data for several compounds which vary substantially with depth in the Cymric oil column, we used equation 2 to determine which portions of the reservoir were yielding the oil produced from wells 1805S and 1815S. The concentration profiles of several such compounds in the extracts and produced oils are shown in Figure 10 for well 1815S and in Figure 11 for well 1805S.

Well 1815S

Oils produced from well 1815S after the first and second cycles of steam injection contained (1) no contribution from below the injection interval (>1538 ft, 469 m); (2) about 85–90% from the middle one-half of the injection interval (1455–1500 ft, 444–457 m); (3) about 10–15% from the upper one-quarter of the injection interval and immediately above the interval (<1450 ft, 442 m).

These conclusions come from solving equation 2 using biomarker data from different combinations of the seven sidewall cores extending from 1570 to 1370 ft (478–418 m) (injection interval = 1420–1538 ft, 433–469 m). For each of the two oils, five such combinations are shown in Table 3; however, only some of these solutions are reasonable because only some of the solutions do not require significant negative contributions from one or more intervals. The oil produced after the second steam cycle appears to contain a somewhat larger contribution from lower in the injection interval (Table 3). Because no data are available for the oil column composition between the sidewall core sampling depths, a precise solution to this allocation problem cannot be expected. Therefore, although we did find a solution to the allocation problem for both oils, we limit our conclusions to the three conclusions listed above. Table 4 lists the biomarker data

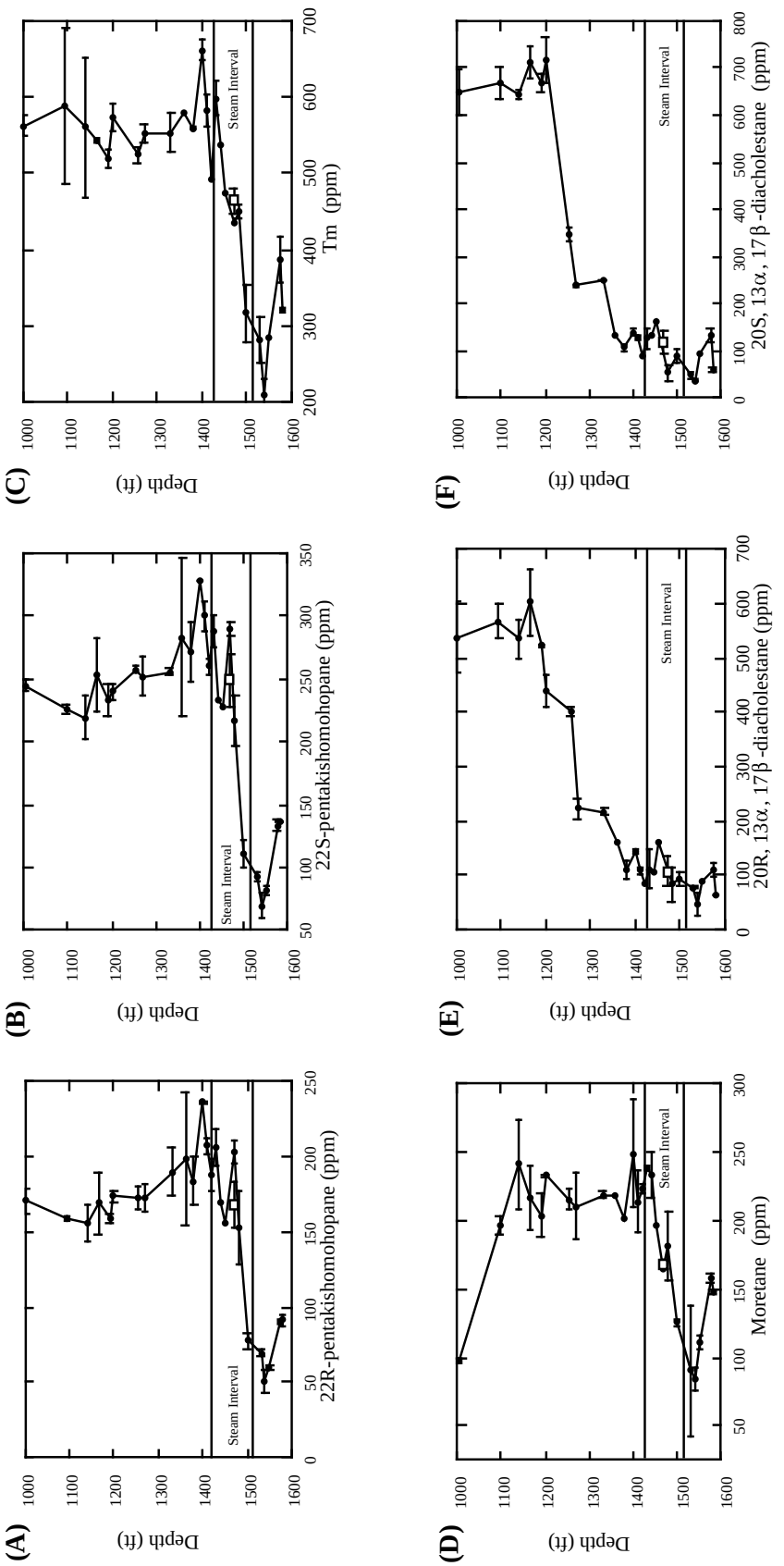

Figure 11—Concentrations (in ppm of saturated hydrocarbon fraction) of six biomarkers in sidewall core extracts (black circles) and produced oil [open square; one per graph, shown at 1470 ft (448 m)] from well 1805S. The steam injection interval is indicated with horizontal bars. Error bars indicate one standard deviation calculated from nonconsecutive duplicate analyses of each sample.

Table 3. Allocation of Produced Oils from Well 1815S*

Sidewall Core Depth (ft)	Contribution to Produced Oil 1				
1350				–0.31	–0.31
1360	**0.11**		0.11	–0.42	–0.43
1430	**–0.02**	**0.09**	–0.03	0.58	0.59
1455	**0.43**	**0.41**	0.31	0.74	0.79
1500	**0.48**	**0.55**	0.76	0.47	0.35
1538		**–0.05**	–0.16	–0.07	
Sidewall Core Depth (ft)	**Contribution to Produced Oil 2**				
1350				–0.27	–0.24
1360	**0.02**		–0.02	–0.44	–0.36
1430	**0.13**	0.17	0.19	0.65	0.55
1455	**0.36**	0.91	0.92	1.10	0.66
1500	**0.48**	–0.82	–0.84	–0.59	0.38
1538		0.74	0.75	0.54	

*For each of the two produced oils, five solutions to equation 2 are shown, one in each column. Each column is an allocation of the produced oil to the sidewall core intervals calculated using different combinations of intervals. Nearly perfect solutions (shown in bold) were found using the compositions of cores from 1360 to 1538 ft (414–469 m). The solutions were derived from equation 2 using the data in Table 4, and were normalized so as to make the contributions from all the zones sum to 1.0.

for the eight compounds used to calculate the solutions in Table 3.

Well 1805S

In well 1805S, the oil produced after the first steam treating of the 1424–1515 ft (434–462 m) interval contained (1) no significant contribution from either below or above the injection interval; (2) no significant contribution from the lower 15 ft (5 m) of the injection interval; (3) as much as 100% derived from the middle 30–50 ft (9–15 m) of the injection interval.

The entire oil column above 1480 ft (451 m) is characterized by high concentrations of both isomers of pentakishomohopane (Figure 11); however, below this depth, the concentrations of these compounds in the oil column decrease by a factor of approximately 3. This transition occurs near the bottom of the zone being steamed. The produced oil, as in the upper three-quarters of the zone being steamed, contains high concentrations of pentakishomohopanes (Figure 11), indicating that very little production is from near the bottom of the zone being injected, and no significant oil production is from below the zone being steam treated. Using equation 2, the abundances of pentakishomohopanes, moretane, and Tm (Figure 11) in the produced oil can be accounted for entirely by a combination of oil from three adjacent sidewall core depths: 1450, 1470, and 1480 ft (442, 448 and 451 m). Furthermore, contributions of these intervals to the produced oils are consistent with the profiles of diacholestanes (Figure 11) in this well, although there are no diacholestane data for one of those sidewall cores. These data suggest that as much as 100% of the produced oil sample was derived from the middle 30–50 ft (9–15 m) of the injection interval. Unfortunately, many other compounds do not show significant variations in concentration across the zone of interest, preventing a more rigorous assessment of the origin of the produced oil.

The relationship between the producing intervals and the steam injection interval is somewhat different in the two wells. This difference probably is the result of a high-permeability fractured chert streak from 1450 to 1460 ft (442–445 m) measured depth in the 1805S well. This high-permeability zone probably acted as a thief zone for the injected steam, and prevented buildup of sufficient pressure to efficiently fracture the lower permeability portions of the interval. The injection intervals in the two wells also differ in that the 1815S interval has substantially more oil in place (8–15 wt. %; Table 1) than does the 1805S interval (1–17 wt. %). Furthermore, there is substantially more variability with depth in the quantity of oil in place in the 1805S steam interval than in the 1815S steam interval (Table 1).

As the steam injection interval is eventually moved to shallower depths, the produced oils should readily be attributable to specific intervals because in both wells a variety of geochemical parameters vary systematically with depth. For instance, in well 1805S, diasteranes in the oil column have relatively constant concentrations from 1000 to 1200 ft (305–366 m), decrease by a factor

Table 4. Biomarker Data Used in Table 3 to Solve Equation 2 for the 1815S Well*

Sample Type	Sidewall	Sidewall	Sidewall	Sidewall	Sidewall	Sidewall	Produced Oil	Produced Oil
Sampling Depth (ft)	1538	1500	1455	1430	1360	1350	1420-1538	1420-1538
GCMS#	B770	B769	B768	B767	B766	B765	B723	B776
Sampling Date	10/11/93	10/11/93	10/11/93	10/11/93	10/11/93	10/11/93	10/17/93	11/11/93
Compound								
30-norhopane	1.00	1.66	3.02	9.93	11.06	7.15	2.63	4.18
Moretane	1.00	1.13	1.66	1.95	3.47	1.19	1.43	1.97
22R,Pentakishomohopane	1.00	2.18	4.30	3.39	4.72	6.81	2.76	3.54
25,30-bisnorhopane	2.44	1.86	1.47	1.00	1.40	2.13	1.57	2.04
22S,25-norhomohopane	2.34	1.94	1.58	1.00	1.29	2.71	1.61	2.28
22R,25-norbishomohopane	3.64	2.74	2.15	1.00	1.66	3.54	2.12	3.12
22S,25-nortrishomohopane	4.46	3.25	2.44	1.00	1.81	3.72	2.29	3.30
22S,25-norpentakishomohopane	11.26	7.04	2.38	1.00	2.32	3.50	3.87	5.22

*For each compound, the concentration in ppm has been divided (i.e., normalized) by the lowest concentration of that compound in the sample set; therefore, the smallest concentration for each compound is listed as 1.00 (no units).

of 6 from 1200 to 1400 ft (366–427 m), and are relatively constant below 1400 ft (427 m) (Figure 11).

Although the wells discussed here are produced by way of steam cycling, the geochemical approach we describe for identifying productive reservoir intervals could also be applied to monitoring the efficiency of a steam or water drive because the compositions of produced oils reflect the composition of the reservoir intervals swept; therefore, such an approach could be used to identify "orphaned oil"; i.e., reservoir intervals either unswept or poorly swept by a flood.

CONCLUSIONS

Development and reservoir management of biodegraded oil accumulations can be optimized by using geochemical indicators of variations in oil biodegradation. In shallow, low-permeability reservoirs, such as the Antelope Shale in the Cymric field, the extent of oil biodegradation can change substantially over vertical distances of just a few feet. These variations can be mapped vertically and laterally using biomarker analyses of oil extracted from sidewall cores. Mapping fieldwide variations in oil biodegradation can yield predictions of lateral and vertical changes in oil producibility. The relationship between oil viscosity and biomarker biodegradation parameters can be calibrated from analyses of produced oils. These relationships can then be used to convert sidewall core biomarker parameters into quantitative predictions of lateral and vertical changes in oil viscosity and gravity. Using these compositional variations, a geologist can assess the relative production volumes from discrete zones and can optimize field development through the choice of (1) well locations and completion intervals, (2) steam injection intervals, and (3) the spacing between injection intervals in the same well.

APPENDIX 1

Equation 2 can be solved readily using the matrix algebra functions (MMULT, MINVERSE, and TRANSPOSE) in Microsoft EXCEL®. For example, to solve the hypothetical problem in Figure 9 using an EXCEL spreadsheet, put matrix G in cells B10:E13, and put matrix d in cells F10:F13. Then select cells B17:B20 for matrix M, and type the following line with no breaks or spaces:

=MMULT(MMULT(MINVERSE(MMULT(TRANSPOSE(B10:E13), B10:E13)),TRANSPOSE(B10:E13)),F10:F13)

into cell B17. Then press COMMAND+SHIFT+RETURN to make B17:B20 an array containing M.

REFERENCES CITED

Baskin, D. K., and R. W. Jones, 1993, Prediction of oil gravity prior to drill-stem testing in Monterey Formation reservoirs, offshore

California: AAPG Bulletin, v. 77, p. 1479–1487.
Colling, E. L., and C. R. Robison, 1991, The variable effects of biodegradation relative to crude oil producibility, *in* R. F. Meyer, ed., Heavy crude and tar sands—hydrocarbons for the 21st century: Caracas, Venezuela, Unitar, v. 2, p. 167–186.
Graham, S. A., and L. A. Williams, 1985, Tectonic, depositional, and diagenetic history of Monterey Formation (Miocene), central San Joaquin basin, California: AAPG Bulletin, v. 69, p. 385–411.
Hughes, W. B., and A. G. Holba, 1988, Relationship between crude oil quality and biomarker patterns, *in* L. Mattavelli and L. Novelli, eds., Advances in organic geochemistry 1987: Organic Geochemistry, v. 13, p. 607–617.
Hunt, J. M., 1995, Petroleum geochemistry and geology: San Francisco, W. H. Freeman, 704 p.
Hwang, R. J., and D. K. Baskin, 1994, Reservoir connectivity and oil homogeneity in a large-scale reservoir: Middle East Petroleum Geoscience, Geo 94, v. 2, p. 529–541.
Hwang, R. J., A. S. Ahmed, and J. M. Moldowan, 1994, Oil composition variation and reservoir continuity: Unity field, Sudan: Organic Geochemistry, v. 21, p. 171–188.
Kaufman, R. L., A. S. Ahmed, and R. J. Elsinger, 1990, Gas chromatography as a development and production tool for fingerprinting oils from individual reservoirs: applications in the Gulf of Mexico, *in* D. Schumaker and B. F. Perkins, eds., Proceedings of the 9th annual research conference of the Society of Economic Paleontologists and Mineralogists, p. 263–282.
Miller, D. E., A. G. Holba, and W. B. Hughes, 1987, Effects of biodegradation on crude oils, *in* R. F. Meyer, ed., Exploration for heavy crude oil and natural bitumen: AAPG Studies in Geology 25, p. 233–241.
Milner, C. W. D., M. A. Rogers, and C. R. Evans, 1977, Petroleum transformations in reservoirs: Journal of Geochemical Exploration, v. 7, p. 101–153.
Moldowan, J. M., and M. A. McCaffrey, 1995, A novel hydrocarbon degradation pathway revealed by hopane demethylation in a petroleum reservoir: Geochimica et Cosmochimica Acta, v. 59, p. 1891–1894.
Moldowan, J. M., C. Y. Lee, P. Sundararaman, R. Salvatori, A. Alajbeg, B. Gjukic, G. J. Demaison, N. E. Slougui, and D. S. Watt, 1992, Source correlation and maturity assessment of select oils and rocks from the Central Adriatic basin (Italy and Yugoslavia), *in* J. M. Moldowan, P. Albrecht, and R. P. Philp, eds., Biological markers in sediments and petroleum: Englewood Cliffs, New Jersey, Prentice Hall, p. 370–401.
Peters, K. E., and J. M. Moldowan, 1991, Effects of source, thermal maturity and biodegradation on the distribution and isomerization of homohopanes in petroleum: Organic Geochemistry, v. 17, p. 47–61.
Peters, K. E., and J. M. Moldowan, 1993, The biomarker guide; interpreting molecular fossils in petroleum and ancient sediments: Englewood Cliffs, New Jersey, Prentice Hall, 363 p.
Peters, K. E., A. E. Kontorovich, B. J. Huizinga, J. M. Moldowan, and C. Y. Lee, 1994, Multiple oil families in the West Siberian basin: AAPG Bulletin, v. 76, p. 893–909.
Requejo, A. G., and H. I. Halpern, 1989, An unusual hopane biodegradation sequence in tar sands from the Pt. Arena (Monterey) Formation: Nature, v. 342, p. 670–673.
Schoell, M., P. D. Jenden, M. A. Beeunas, and D. D. Coleman, 1993, Isotope analysis of gases in gas field and gas storage operations: Society of Petroleum Engineers, no. 26171, p. 337–344.
Seifert, W. K., and J. M. Moldowan, 1979, The effect of biodegradation on steranes and terpanes in crude oils: Geochimica et Cosmochimica Acta, v. 43, p. 111–126.
Thompson, K. F. M., 1987, Fractionated aromatic petroleums and the generation of gas-condensates: Organic Geochemistry, v. 11, p. 573–590.
Volkman, J. K., R. Alexander, R. I. Kagi, and G. W. Woodhouse, 1983, Demethylated hopanes in crude oils and their applications in petroleum geochemistry: Geochimica et Cosmochimica Acta, v. 47, p. 785–794.

ABOUT THE AUTHORS

Mark A. McCaffrey

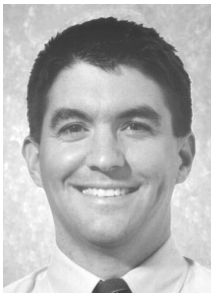

Mark McCaffrey is a senior research geochemist at ARCO Exploration Production Technology in Plano, Texas, where he works on oil exploration and production problems. Mark was the 1995 recipient of the Pieter Schenck Award from the European Association of Organic Geochemists for "outstanding work on biomarkers in relation to paleoenvironmental studies and petroleum exploration." A California Registered Geologist, he received his B.A. degree (1985) from Harvard University, magna cum laude with highest honors in geological sciences, and his Ph.D. (1990) in oceanography from the Massachusetts Institute of Technology/Woods Hole Oceanographic Institution Joint Program.

Henry A. Legarre

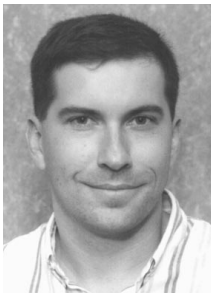

Henry Legarre is a research geologist with Chevron Petroleum Technology Company in La Habra, California. He received his M.S. degree from San Diego State University, California, in geological sciences. As a development geologist with Chevron USA, he worked on reservoir development and modeling and consulted on a variety of domestic and international projects. Previously employed by Scripps Institute of Oceanography and Woods Hole Oceanographic Institution, Henry's research has involved organic and inorganic geochemistry, clay mineralogy, hydrogeology, clastic diagenesis, and surface ocean biogeochemical processes.

Scott J. Johnson

Scott Johnson has been a development geologist with Chevron USA in Bakersfield, California, since 1991. Assignments have involved the Santa Barbara Channel, the onshore and offshore Santa Maria basins, the Los Angeles basin, and the Lost Hills and Cymric fields. He graduated Phi Beta Kappa with a B.A. degree in geology from the University of Colorado in 1985. He received an M.S. degree in geology from Northern Arizona University in 1991. He has published on topics including syntectonic sedimentation and borehole imaging.